



Article

Optimization of Wire-EDM Process Parameters for Al-Mg-0.6Si-0.35Fe/15%RHA/5%Cu Hybrid Metal Matrix Composite Using TOPSIS: Processing and Characterizations

Jatinder Kumar ^{1,*}, Shubham Sharma ^{2,3,*}, Jujhar Singh ², Sunpreet Singh ⁴ and Gurminder Singh ⁵

¹ Department of Mechanical Engineering, St. Soldier Institute of Engineering and Technology, Jalandhar 144011, India

² Department of Mechanical Engineering, IKG Punjab Technical University, Kapurthala 144603, India

³ Mechanical Engineering Department, University Centre of Research and Development, Chandigarh University, Sahibzada Ajit Singh Nagar 140413, India

⁴ Department of Mechanical Engineering, National University of Singapore, Singapore 119077, Singapore

⁵ Department of Mechanical Engineering, Indian Institute of Technology Bombay, IIT-Bombay, Mumbai 400076, India

* Correspondence: jatinderbahal@gmail.com (J.K.); shubham543sharma@gmail.com (S.S.)

Abstract: The current experimental study concerns obtaining the optimal set of wire-EDM processing factors for a novel Al-Mg-0.6Si-0.35Fe/15%RHA/5%Cu hybrid aluminum matrix composite. The composite exhibits hardness of 64.2 HRB, tensile strength 104.6 MPa, impact energy 4.8 joules, when tested using standard testing techniques. For this, composite is formulated with the help of a stir casting route. The tests are conducted as per Taguchi's L_{27} OA, to explore the influence of processing factors on the surface roughness (Ra), radial overcut (ROC) and material removal rate (MRR). The optimization is executed using the Taguchi approach, followed by multiple objective optimizations with TOPSIS (one of the MADM techniques). For optimal values of Ra, MRR and ROC, the optimum set of input variables is suggested as 150 A of current, 125 μ s of pulse duration, 50 μ s of pulse interval and 8 mm/min of wire feed-rate. Predicted performance index value was calculated and was compared with the experiment value. It has been observed that both values are very close to each other with only 1.33% error, which means the results are validated. ANOVA confirms that current is a predominant factor influencing response characteristic parameters, which contributes 24.09%, followed by pulse duration (16.78%) and pulse interval (15.18%). The surface characterization using a scanning electron microscope (SEM), X-ray diffraction (XRD), energy dispersive spectroscope (EDS) and optical microscope (OM) has also been carried out to affirm the existence of the reinforcing particles in the base matrix.

Keywords: TOPSIS; composite; RHA; stir casting; surface roughness



Citation: Kumar, J.; Sharma, S.; Singh, J.; Singh, S.; Singh, G. Optimization of Wire-EDM Process Parameters for Al-Mg-0.6Si-0.35Fe/15%RHA/5%Cu Hybrid Metal Matrix Composite Using TOPSIS: Processing and Characterizations. *J. Manuf. Mater. Process.* **2022**, *6*, 150. <https://doi.org/10.3390/jmmp6060150>

Academic Editor: Steven Y. Liang

Received: 8 September 2022

Accepted: 17 November 2022

Published: 22 November 2022

Publisher's Note: MDPI stays neutral with regard to jurisdictional claims in published maps and institutional affiliations.



Copyright: © 2022 by the authors. Licensee MDPI, Basel, Switzerland. This article is an open access article distributed under the terms and conditions of the Creative Commons Attribution (CC BY) license (<https://creativecommons.org/licenses/by/4.0/>).

1. Introduction

Composite materials consist of at least two constituent materials with substantially different properties, which remain separate and the finished structure is distinct on a macroscopic level. Many researchers have reported their valuable past work activities related to the manufacture and machining of composite materials. Reduced weight, high-strength and high-toughness materials for applications such as aerospace, automotive and nuclear industries have been produced with the latest technologies.

Recent developments in the manufacturing industry have fueled the demand for materials having higher strength, hardness and toughness. These materials pose a problem while machining with the conventional machines available. The new materials available are lightweight, combined with greater hardness and toughness. Sometimes their properties may create major challenges during their machining. Therefore, non-conventional methods

of machining, including electrochemical machining (ECM), ultrasonic machining (USM), electrical discharging machine (EDM), the newly developed hybrid machining, etc., refer to machine materials that are difficult to process. WEDM is the most generalized machine tool for machining such materials. Wire-EDM is a process used to cut a conductive material with a thin wire electrode (usually brass) following a direction regulated by the CNC. WEDM leaves on the surface a very random pattern compared to other conventional milling cutters and grinding wheels.

The wire-EDM is used to manufacture complex forms in two or three dimensions, using a simple wire that erodes the material from an electrically conductive material. Wire-EDM also called an electric discharge wire cutting machining process. This process is best suited for cutting any kind of hard and conductive material. In this process, a brass or copper wire is used as electrode material. With wire motion speeds up to 3 m/min with respect to the work material, a spark is generated, resulting in erosion, and thus the material is removed. It uses a CNC controlled machine set up for machining. Philip Koshy et al. [1] determined that the provision of holes in the electrode is unworkable; a major issue is the flushing of the working distance. The efficient flushing at the working gap, generated by rotation of the electrodes, dramatically enhanced MRR along with surface finishing. Hung et al. [2] explored the possibility of implementing electric discharge machining for SiC-AMCs. It was indicated that SiC particles have a negative impact on MRR. It is because the aluminum matrix is insulated and covered by these particles from being vaporized. Coupled with surrounding molten aluminum droplets, the un-melted SiC fall down the composite material. Tarng et al. [3] evaluated the optimum cutting parameters for improving the cutting efficiency in WEDM. A feed forward style neural network (NN) is used to co-relate cutting output to the input variables. The NN is then subjected to a convex optimization algorithm in order to solve the optimum input parameters based on an efficiency index. The results indicated that WEDM's cutting efficiency with this new method can be greatly enhanced. Che Chung Wang and Biing Hwa Yan [4] conducted a study to optimize Al₂O₃/6061 Al blind hole drilling using rotary electrode discharge machining. Results showed that in contrast to stationary solid electrodes and rotary solid electrodes with injection flushing, the Cu electrode with an eccentric hole performs best among others. Rozenek et al. [5] explored the impact of machining factors during Al-Si7Mg/SiC-MMC and AlSi7Mg/Al₂O₃ composite electrical discharge machining. The analysis found that machining of composites relies on the type of reinforcement used. The cutting speed of Al-SiC and Al-Al₂O₃ composites is approximately three times slower than that of the aluminum alloy. Mahapatra and Amar Patnaik [6] prepared a model to modify the input variables for wire-EDM. Results indicated that the responses were influenced significantly with respect to the input variables. Fuzhu et al. [7] examined the impact of input factors of wire-EDM on surface quality. It was indicated that Ra is improved by reducing the pulse length and discharge current. Yan et al. [8] studied EDM process development using a standard EDM machine assisted by magnetic force. The consequences of magnetic force on features of EDM machining were determined. This concluded that EDM aided by magnetic force has a superior MRR and relatively inferior EWR and Ra than a normal EDM. Often calculated are the important machining parameters and the optimum combination rate of both MRR and Ra machining parameters associated with them. Mohammad Zadeh et al. [9] conducted an experiment using MWCNTs mixed dielectric to improve the effectiveness of EDM together with copper electrodes while machining H13 tool steel. The study found that mixing MWCNTs inside the dielectric improves EDM efficiency at lower levels of pulse off energy. Khalid and Kuppan [10] studied the impact of mixing of Al powder in the dielectric fluid (distilled water) during machining of die steel. The tool and work electrode materials used were, respectively, electrolytic copper and W300 die steel. This research concluded that the lower white layer with a thickness of 17.14 µm was obtained at a high 4 g/L powder concentration and low 6 A peak current. Kannachai and Prajak [11] conducted a study to examine an optimal cutting condition to implement dimensional accuracy and Ra in the WEDM-ed K460 tool steel finish cutting process. It was ascertained that both offset distance

and current affect the sample dimension significantly, while current alone affects the Ra. It was concluded that the optimal cutting condition is at 772 μm offset distance and at 2 A peak current. Chin Chang et al. [12] explored surface morphology of a polycrystalline silicone ingot while machining it with wire-EDM. It indicated that the mixing of pure water with $\text{Na}_4\text{P}_2\text{O}_7$ powder has significantly better process efficiency and surface smoothness. Rajesha et al. [13] found that a minimum recast layer Ra during WEDM for Al 7075 MMCs is obtained with gap current 15 A, pulse duration 10 μs and pulse interval 6 μs . Jangra et al. [14] studied the sophisticated machining of WC-5.3%Co MMC using wire-EDM. In order to simultaneously standardize the four mechanical parameters, ANOVA shows that taper angle, pulse duration and pulse interval are important parameters determining the MRR and Ra. For radial overcut, the parameters, such as taper angle, peak current and pulse duration, are the predominant factors, and for angular error, parameters such as angle, current and flow rate were considered as significant factors.

Akash et al. [15] utilized refinery industry waste alumina as reinforcement to formulate aluminum matrix composites. The composition of alumina varied at 0, 5 and 10% by weight and was formulated through a powder metallurgy process. The authors observed that a composite casting containing 5% alumina possessed maximum hardness (25 HRH) and compressive strength (22 MPa), while 10% alumina-based composite possessed 19 HRH, 12 MPa, respectively, and pure aluminum exhibited 17 HRH and 10 MPa, respectively. The authors concluded that a composite formulated from waste material can withstand more load than the base matrix. Joseph et al. [16] used MoS_2 (solid lubricant) as reinforcement to develop an aluminum 6063 alloy metal matrix composite. The composition of MoS_2 was varied at 0, 5 and 10% and composites were formulated through a powder metallurgy route. The authors observed a significant reduction in wear rate with the addition of MoS_2 constituents due to the lamellar crystalline structure. The authors also reported from SEM images that abrasive and adhesive type wear mechanisms occurred. Ho and Newman [17] claimed that electric discharge machining's (EDM) introduction to metal cutting was a realistic machining method to produce highly complex pieces, irrespective of the mechanical properties of workpiece materials. Mainly because of the dynamic behavior of the sparking factor in determining parameters of both electrical and non-electrical processes, the managing of the electric discharge machining (EDM) mechanism depended on empirical methods. The electric discharge machining (EDM) method has to be continuously revitalized in order to stay competitive in maintaining an important and useful role in the manufacture of component tool rooms with hard-to-machine materials and shapes.

Shu et al. [18] commissioned a survey exploring the influence of silicon carbide particle size and electrode rotational velocity on HPM50 mold steel's EDMG. Researchers indicated that EDMG could obtain high MRR when selecting an appropriate electrode, rotational velocity, silicon carbide particle size and current. Simao et al. [19] conducted an experiment using EDM to establish the surface modifier. Descriptions of the exercises included powder metallurgy device electrodes and the use of dielectric fluid suspending powders, usually aluminum, titanium, nickel, etc. The research results of this study were found using partially annealed WC/Co electrodes working in a dielectric hydrocarbon oil on the surface alloy of AISI H13 hot work tool steel during a die sink process. Aharwal et al. [20] conducted a study to examine the microstructure of Al SiC composite after use of EDM for machining it. The best silicon content found in the constituent is 10 per cent, and the hardness thus obtained makes it suitable for die making. Experiments for data collection and classification of selected output parameters were conducted using linear regression analysis. For machine operators, this is useful in selecting the optimum input parameters, which optimize MRR and SR. In the field of data analysis, more research in this area can be achieved by considering multi-objective optimization as users may be concerned about maximum value of both material removal rate (MRR) and surface roughness (SR).

Onoro [21] conducted a study of the tensile properties and fracture properties of composites strengthened by TiB_2 . These materials were investigated at room temp. and at

high temps. for the identification of ultimate strength and strain to failure. An enhancement in the physicomaterial behavior was attained by incorporating TiB_2 particles in both the Al alloys as reinforcement. The research concluded that adding TiB_2 particles decreases the ductility of the Al alloys but does not change the microscopic failure mechanism, and the surface of the fracture exhibits a ductile impression with coalescence-formed dimples.

Vishal et al. [22] conducted a study proposing the complex DoE of a Taguchi for optimizing Ra in WEDM. Experiments were planned according to the mixed OA of Taguchi's L32. In the test, under different cutting conditions, each experiment was performed with gap voltage, pulse-off time and pulse-on time, wire feed and dielectric flushing pressure. The chosen working material for performing the experiments was grade 304 L stainless steel. The Ra for each machining efficiency parameter was determined from experimental tests. The performance characteristics deviating from the actual value S/N ratio were added to measure. Finally, experimental tests were performed to assess the feasibility of the approach proposed. Saha et al. [23] researched the dry EDM cycle with an electrode tubular copper device and a mild steel workpiece. In this research, experiments were performed using air and the effect on TWR, MRR and SR of the gap voltage discharge current, duty factor, Pon-time, air pressure, and spindle speed was tested. ANOVA experiments were used to classify the parameters that were important. The dry EDM attachment showed the experimental result and it was found that MRR and SR (Ra) are influenced by the flow characteristic of air in the inter-electrode distance. The device has an acceptable number of airflow openings, so the Ra is the lowest and the MRR is the largest. Mahdavinejad [24] conducted a study that uses the neural model predictive control method to present optimization and control of the EDM process. The test results from WC-Co's EDM confirm the potential of the NN-based predictive controller model system with an improvement in stock removal rate of 32.8 per cent output. The analysis between the setup obtained on EDM through the machine and the expert user was carried out with 8 h of machining. The NN-based predictive controller system was designed and developed regarding the EDM parameters on carbon-based materials and the results of testing performed on WC-Co using an electrodischarge die sinking machine were found. From the analysis results, it was found that WC-Co's EDM confirms the NN-based predictive controller model device's capability with an efficiency of 32.8 per cent.

Patel Gowdru Chandrashekarappa et al. [25] performed a comparative study during machining of HCHCr steel with electric discharging machining. The objective of the study was to reduce tool wear rate and surface roughness and increase cutting rate. The authors utilized Cu, Gr and brass as electrode materials, distilled water and kerosene oil as dielectric fluids, peak current and pulse interval as input parameters. The authors used Taguchi coupled CRITIC Utility and Taguchi coupled PCA Utility techniques to predict the optimal set of input conditions. The authors reported that maximum MRR = 0.063 g/min and minimum surface roughness = 1.68 μm and tool wear rate = 0.012 g/min were obtained with a graphite tool when machining was performed under distilled water. Sen et al. [26] utilized the trapezoidal interval type-2 fuzzy number integrated analytical hierarchy process-based additive ratio assessment approach for predicting the best wire-EDM process parameters during machining of Inconel-800 alloy and the findings were compared with one of the MADM techniques to validate the obtained results to confirm the applicability of the projected method. The authors reported that the used approach is best suited for problem formulation and assessing and ranking of wire-ESM process parameters. The conditions of input variables suggested by the current approach are pulse duration of 105 μs , pulse interval of 57 μs , current of 210 A, voltage of 50 v. Aggarwal et al. [27] explored the machining behavior of Monel K-500 alloy in the form of material removal rate and surface roughness using wire-EDM. The authors performed experiments according to central composite design and analyzed using response surface methodology. Pulse duration, pulse interval, wire feed rate and voltage were selected as input parameters to explore their effect on the response parameters. The authors noticed that MRR and surface roughness vary proportionally with respect to pulse duration and inversely with respect to pulse

interval. Both MRR and surface roughness were reduced with an increase in voltage. The optimal values of MRR and surface roughness obtained through gray relational analysis were 2.480 mm/min and 2.12 μm , respectively.

Kumar et al. [28] explored the microstructure and characteristic properties and machining behavior of Al-SiC-Mo composites, which were fabricated through a stir casting route. During fabrication, composition of silicon carbide was kept constant, while molybdenum was varied from 0 to 4 with steps of 2. The authors reported that microstructure was refined with the addition of Mo together with SiC in the aluminum alloy. The authors also observed a significant improvement in strength, hardness and wear resistance with the inclusion of reinforcement particulates in the base aluminum alloy. During turning of newly developed composites, the authors observed that speed, feed and interactions between them are predominant factors effecting surface roughness and the composition of Mo shows a minor effect on it. Similarly, cutting depth shows a significant effect on MRR.

Kumar et al. [29] performed a comparative study of properties and metallographic studies of Al-SiC-Cr hybrid composites and the results were compared with the base matrix and composite containing SiC only as a reinforcing agent. The authors followed a vortex casting route during fabrication. During fabrication, the composition of silicon carbide was kept constant, while chromium was varied from 0 to 3 in steps of 1.5. The authors observed that hardness and wear resistance were improved significantly, but with a smaller reduction in strength than Al-SiC composite, however, the obtained strength was higher than that of unreinforced aluminum alloy. The authors also observed the formation of chromium carbide resulting from the internal reaction between the constituents. A tree-like dendritic structure was also observed in Al-SiC-Cr hybrid composites.

Based on the observations made from an exhaustive literature survey, it has been noticed that limited work has been carried out to produce high-quality and low-cost reinforcements from industrial and agricultural wastes. The bulk of the recorded work relates to SiC-AMCs, and it is likely that less work has been carried out on rice husk-reinforced AMCs. Very limited work has been carried out to achieve high MRR for controllable input variables such as current, pulse duration, pulse interval, wire feed rate, etc. So, the objective of this study is formulating an Al/RHA/Cu hybrid composite through stir casting, and exploring the behavior of wire electric discharge machining characteristics during machining and proposing a set of optimized effective input variables to obtain optimal responses in the form of MRR, surface finishing and dimensional accuracy. For this, an L_{27} orthogonal array is adopted to perform tests and the optimization method including the Taguchi method, followed by TOPSIS, was used to investigate which process parameters are optimally set.

2. Materials and Methods

2.1. Materials

Aluminum–silicon (Al-Mg-0.6Si-0.35Fe) alloy was chosen for this study. This alloy exhibits many applications in automotive components such as piston, cylinder liner, etc. The required weight of aluminum was cut from the ingot and recast in the desired shape using stir casting. For this experiment, Al-Mg-0.6Si-0.35Fe was used as matrix material and rice husk ash (RHA) and copper (Cu) by weight were chosen as reinforcements. Using the stir casting process, rice husk ash was used to prepare the reinforcing step with Al-Mg-0.6Si-0.35Fe alloy as the matrix. To increase the wettability among constituents, 1 wt. % of Mg was also introduced in the molten metal.

The images of scanning electron microscopy (SEM) and energy dispersive spectroscopy (EDS) are shown in Figure 1. The highest Al peak in EDS depicts that aluminum is a main constituent of the alloy while the peak of Si reveals that Si is a major alloying element in it. Other peaks in the EDS image show the existence of other alloying elements within the Al alloy. The optical micrograph of aluminum alloy is shown in Figure 2 [28,29].

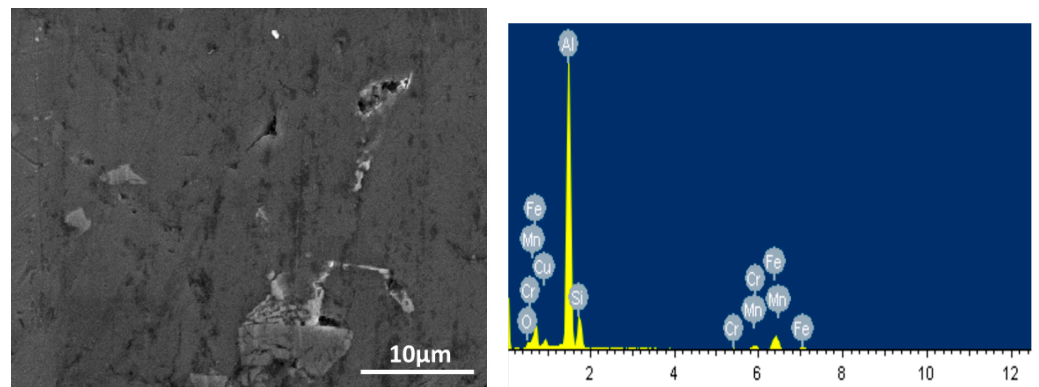


Figure 1. SEM (at 2000×) and EDS images of base Al-Mg-0.6Si-0.35Fe alloy matrix.

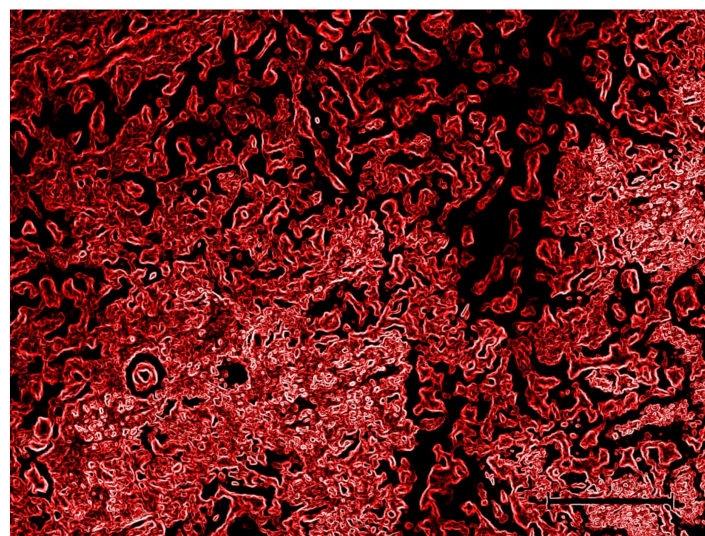


Figure 2. Optical micrograph of base Al-Mg-0.6Si-0.35Fe alloy matrix.

Microhardness was evaluated using a Rockwell hardness tester, a tensile test was conducted on a UTM, a pin-on-disc wear test was used to measure wear rate, porosity level was estimated with the help of Mattler Toledo apparatus and a scratch test was conducted on a scratch adhesion machine. All of the properties were evaluated as per ASTM standards using advance testing techniques, and the results are listed in Table 1.

Table 1. Properties of base Al-Mg-0.6Si-0.35Fe alloy matrix.

S. No.	Property	Value
1	Microhardness (HRB)	42
2	Ultimate tensile strength	82 MPa
3	Percentage elongation	7.52%
4	Wear rate	2.032 mm ³ /min
5	Friction coefficient	0.139
6	Theoretical density	2.685 g/cm ³
7	Actual density	2.684 g/cm ³
8	Percentage porosity	0.025
9	Traction force	8.46 N

2.2. Preparation of Rice Husk Ash (RHA)

Rice husk was rinsed with water to remove its dust and other unwanted items, and dried at room temperature. The rice husk was further put into a crucible of graphite and

heated for one hour up to 240 °C to extract its moisture and organic matter for spectacular results. The color of the rice husk changed from yellowish to black due to the presence of organic matter during this heating process. The rice husk was heated up to 660 ± 20 °C for 5 h and the rice husk was completely burnt due to the presence of oxygen. The ash was further heated in an electric furnace at 750 °C for 10 h to obtain desired properties. Once this operation was completed, at room temperature, the color of the ash shifted thoroughly from black to gray or slightly grayish-white. The microstructural and composition analysis of RHA powder was conducted by SEM in conjunction with EDS in order to analyze the morphological characterizations. Test results reveal that the silica particulates (SiO_2) were dispersed across micrographs and scattered uniformly as shown in Figure 3. The EDS spectrum indicates peaks of Ca, C, K, O, Si, P, etc. and the presence of oxygen confirms the presence of Al_2O_3 , SiO_2 and potassium oxide.

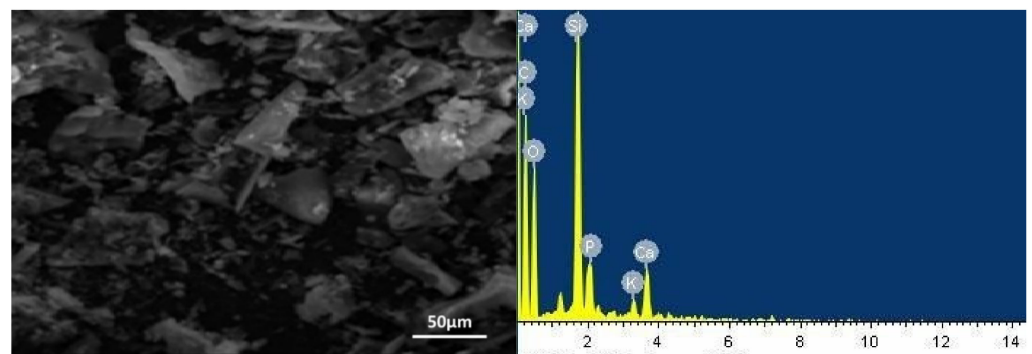


Figure 3. SEM (at 500 \times) and EDS image of RHA.

Figure 4 depicts the phases occurring in RHA, cristobalite and quartz. Intense XRD patterns of RHA at 2-theta values of 20.4°, 21.8°, 28°, 31.2° and 35.8° imply cristobalite silica, whereas 20.8° and 26.6° signify quartz silica [30]. Moreover, with the aid of such identified peak positions, one can find any peak that may be induced through a creation of inter-metallic compounds throughout sintering [30].

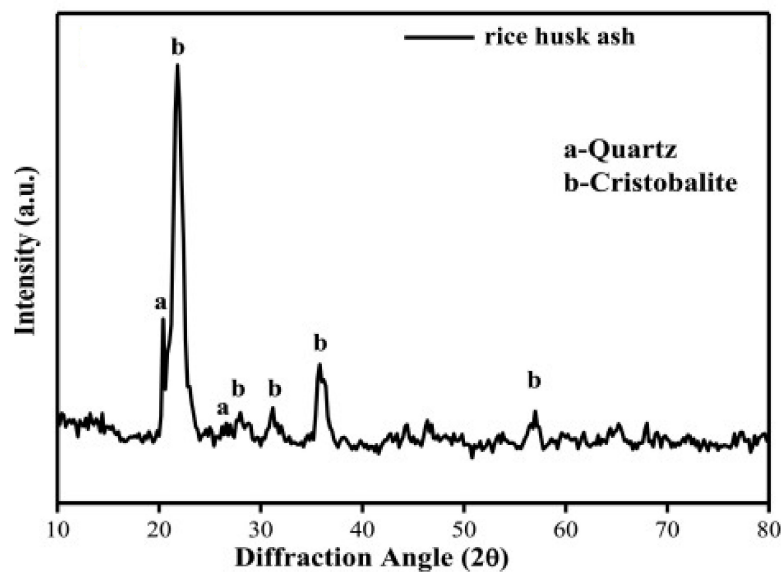


Figure 4. X-ray diffraction pattern of RHA. Adapted from the reference [30].

2.3. Composite Preparation

There was use of a two-step stir casting technique in this composition for its processing. Around a temperature of 240 °C, the RHA and copper particles were initially preheated

differently to eliminate moisture and increase wettability with molten aluminum alloy. The matrix alloy was charged in graphite crucible and melted by an electric furnace at around 740 °C. In the furnace, the liquid content melted to a semi-solid state at about 650 °C. Rice husk ash (RHA) and copper (Cu) particles were charged to the semi-solid melt at 620 °C and stirred sequentially for up to 15 min. To increase the wettability between the matrix and reinforcement, 1% magnesium was added. The semi-solid hybrid composite combination was heated to around 850 °C and stirred at 370 rpm for 10–12 min by means of an automated mechanical stirrer. Ultimately, for casting, the molten plastic mixture was poured into a steel mold and allowed to solidify at room temperature.

The composite exhibited hardness of 64.2 HRB, tensile strength 104.6 MPa, impact energy 4.8 joules, when tested using standard testing techniques.

The scanning electron microscopy (SEM) and energy dispersive spectroscopy (EDS) images of the novel composite are shown in Figure 5.

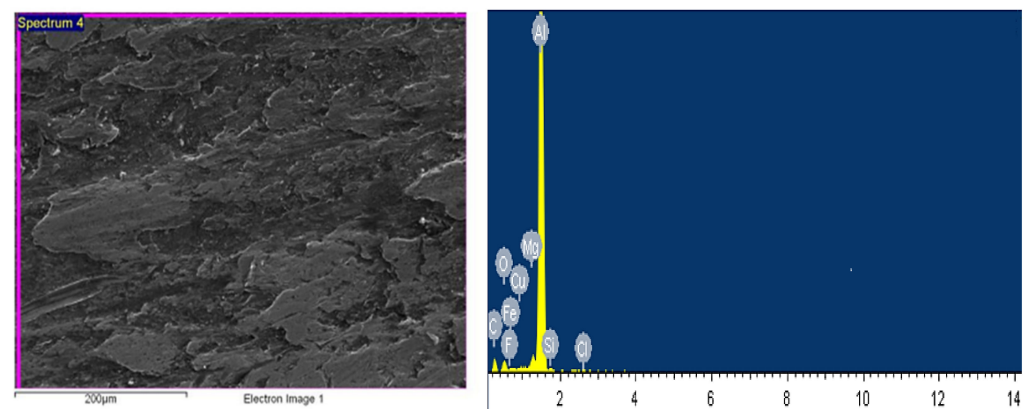


Figure 5. SEM and EDS images of Al-Mg-0.6Si-0.35Fe/15%RHA/5%Cu hybrid composite workpiece before machining.

2.4. Physicomechanical Characteristics

Tensile tests were conducted on as-cast composite samples according to ASTM standards using a universal testing machine. In order to test the reliability of the data generated from each composite composition, four samples were evaluated at room temperature and an average value was taken for further analysis. A test specimen's ultimate tensile strength and percentage elongation can be measured and evaluated based on the test data. The hardness test of the prepared specimens was conducted in standard test conditions according to the B scale using a "Rockwell hardness testing machine". For this hardness test, the samples need to be machined and polished in order to achieve a smooth, plane surface. To obtain reliable results, four readings were taken for each sample, and an average value was determined as a measure of the specimen's hardness. The Charpy impact test technique was used to determine the impact strength (toughness) of the composites. ASTM standards were used to prepare the composite specimens for the Charpy impact test arrangement ($10 \times 10 \times 55 \text{ mm}^3$). For reliability, notched samples were tested at room temperature and at four different temperatures for each composite composition, then averages were calculated.

2.5. Composite Machining

The experiments were conducted on an automatic "Electronica Sprintcut" CNC wired electrical discharge machine (WEDM) installed at "Hindustan New Tools" in Jalandhar, Punjab, India, which is 4-axis computer numerical control (CNC) as exhibited in Figure 6. These four axes' movements were similarly controlled by a four-closed-loop DC motor system. The prominent specifications of the WEDM are illustrated in Table 2.



Figure 6. (a,b) Illustration of wire-EDM during machining.

Table 2. The specifications of wire-EDM.

S.No.	Parameters	Values
1.	Maximum table size	440 × 650 mm
2.	Maximum workpiece height	200 mm
3.	Maximum workpiece weight	300 kg
4.	Main table transverse (X, Y)	300 × 400 mm
5.	Maximum taper cutting angle	±300/50 mm
6.	Maximum cutting speed	160 mm ² /min
7.	Wire diameter	0.25 mm, Brass
8.	Generator	ELPULS-40 A DLX
9.	Controlled axes	X, Y, U, V simultaneous/independent
10.	Auxiliary table traverse (u, v)	80 × 80 mm

The presence of massive wreckage and deep craters on the surface of some specimens after machining can be seen in SEM micrographs. A high discharge current value may be the cause of this. During EDM, higher discharge energy generates higher temperatures at the spark stage, causing material to melt and evaporate. The melted material that was not adequately flushed away from the surface solidifies again, resulting in a rougher surface [31,32]. At higher discharge current and pulse-on time speeds, more discharge energy is available, resulting in the creation of large craters, microcracks and debris. The SEM micrographs are used to visualize large deep craters and rubble. A comparison of micrographs from Figure 7a,b revealed that at higher discharge currents, deep craters and microholes are likely, making the surface rougher. Furthermore, it is apparent that the substance has been melted, followed by washing out of the molten material. A large portion of the heat produced is dissipated in the machining area at a lower discharge current speed [31,33,34]. As a result, less pulse energy is used to melt and vaporize the workpiece. As a result, shallow craters form on the machined surfaces, as seen in Figure 7a,b. The longer the pulse-on time, the less efficient the machining. The machined surface is thus present, along with a wavy surface and bubbles formed during the pulse-off time due to plasma collapse.

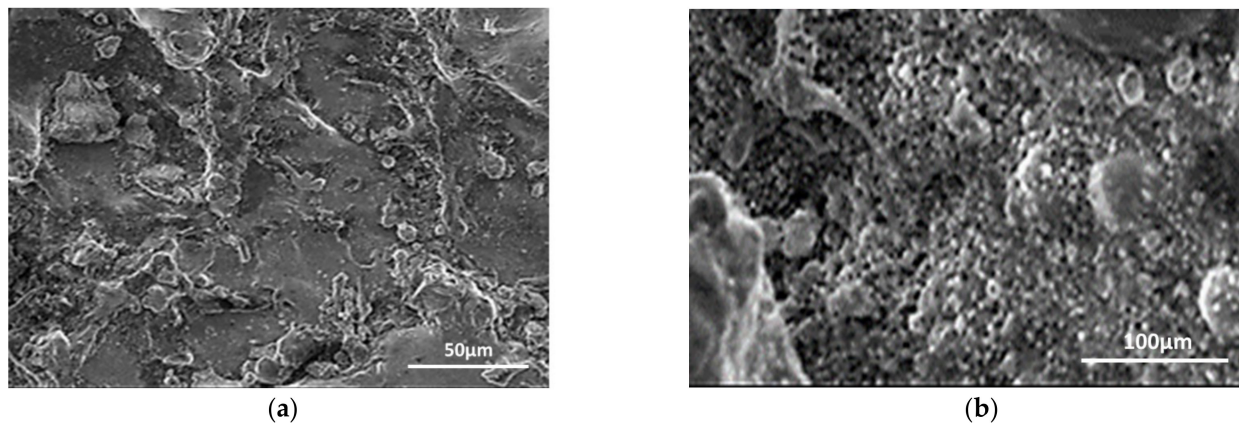


Figure 7. SEM of Al-Mg-0.6Si-0.35Fe/15%RHA/5%Cu hybrid metal matrix composite workpiece at (a) $\times 500$ and (b) $\times 250$ res. after wire-EDM.

2.6. Design of Experiments

In the Taguchi experimental design, different levels of process parameters were chosen as the per literature survey and pilot study. The experiments were performed according to L_{27} OA. Machining characteristics of the hybrid composite were evaluated based on the output responses such as MRR, Ra and ROC. For the present experimental work, four input parameters were chosen and their levels are listed in Table 3.

Table 3. Input factors with levels.

Factors	Units	Level-I	Level-II	Level-III
Peak current (I_p)	Ampere	100	150	200
Pulse duration (T_{On})	μs	115	125	135
Pulse-off time (T_{Off})	μs	30	40	50
Wire feed rate (W_f)	m/sec	3	8	13

The MRR was calculated from the observational data collected at the time of experimentation. The workpiece was adequately washed and disinfected before weighing, for protection from dust particles. Workpiece weights, prior to and after machining, were recorded using a high-precision digital weighing machine and the weight difference gave the workpiece weight loss during the machining. MRR is expressed as the ratio of the workpiece's weight difference to the time taken and is calculated according to Equation (1).

$$MRR = \frac{w_b - w_a}{t}, \quad (1)$$

where, before and after machining, " w_b " and " w_a " are weight of work material, and " t " is the machining time.

The overcut measured after wire-EDM indicated the dimensional accuracy of the process. For this, the cut gap was measured after each run using an instrumental profile projector. The surface roughness was found using a Talysurf roughness tester. For accuracy, three readings per sample were noted and their average was taken for analysis. Table 4 represents the control log of experiments and corresponding response parameters.

The optimization was performed by the Taguchi method using Minitab 18 software. Multiple objective optimizations were also performed using one of the multiple attribute decision-making (MADM) techniques.

Table 4. Control log of experiment and corresponding responses.

Run No	I _p (A)	P _{on} (μs)	P _{off} (μs)	W _f (mm/min)	Ra (μm)	MRR (g/min)	ROC (mm)
1	100	115	30	3	0.11	0.19176	0.007
2	100	115	40	8	0.10	0.28691	0.012
3	100	115	50	13	0.11	0.36955	0.022
4	100	125	30	8	0.11	0.34404	0.017
5	100	125	40	13	0.15	0.48130	0.029
6	100	125	50	3	0.19	0.60053	0.018
7	100	135	30	13	0.18	0.42390	0.036
8	100	135	40	3	0.17	0.64174	0.029
9	100	135	50	8	0.19	0.91845	0.037
10	150	115	30	8	0.15	0.27773	0.021
11	150	115	40	13	0.13	0.43568	0.013
12	150	115	50	8	0.11	0.55433	0.027
13	150	125	30	13	0.13	0.49455	0.018
14	150	125	40	3	0.13	0.67949	0.034
15	150	125	50	13	0.14	0.96084	0.050
16	150	135	30	3	0.15	0.61955	0.041
17	150	135	40	8	0.16	0.88856	0.058
18	150	135	50	8	0.09	1.33593	0.034
19	200	115	30	13	0.22	0.35018	0.028
20	200	115	40	8	0.17	0.56015	0.056
21	200	115	50	13	0.23	0.72063	0.033
22	200	125	30	3	0.11	0.65940	0.061
23	200	125	40	13	0.18	0.88856	0.039
24	200	125	50	3	0.20	1.20105	0.057
25	200	135	30	8	0.15	0.73219	0.046
26	200	135	40	8	0.19	1.28348	0.065
27	200	135	50	13	0.13	1.83690	0.098

TOPSIS is one of the MADM techniques, used for multiple objective optimizations. This technique suggests one common setting and two artificial alternatives. The procedure involved is:

Step I—Establish decision-making matrix.

$$\begin{matrix}
 x_{11} & x_{12} & \dots & x_{1n} \\
 x_{21} & x_{22} & \dots & x_{2n} \\
 \dots & \dots & \dots & \dots \\
 x_{m1} & x_{m2} & \dots & x_{mn}
 \end{matrix}$$

Step II—Build a normalized decision matrix. Normalized data are obtained using Equation (2).

$$R_{ij} = \frac{x_{ij}}{\sqrt{\sum_1^m x_{ij}^2}} \text{ where } i = 1, 2, \dots, m \text{ and } j = 1, 2, \dots, n \tag{2}$$

Step III—Construct a weighted normalized decision matrix using Equation (3).

$$V_{ij} = R_{ij} \times W_j \tag{3}$$

Step IV—Identify PIS and NIS using Equations (4) and (5).

$$PIS = A^+ = \{V_1^+, V_2^+, V_3^+ \dots V_n^+\}, \text{ where } V_j^+ = \{(maxi(V_{ij}) \text{ if } j \in J); (mini(V_{ij}) \text{ if } j \in J')\}, \tag{4}$$

$$NIS = A^- = \{V_1^-, V_2^-, V_3^- \dots V_n^-\}, \text{ where } V_j^- = \{(mini(V_{ij}) \text{ if } j \in J); (maxi(V_{ij}) \text{ if } j \in J')\}, \tag{5}$$

where *J* represents a favorable attribute and *J'* represents the unfavorable attributes.

Step V—Calculate the separation distances using Equations (6) and (7).

$$S^+ = \sqrt{\sum_{j=1}^n (V_j^+ - V_{ij})^2} \quad \text{where } i = 1, 2, 3, \dots, m, \tag{6}$$

$$S^- = \sqrt{\sum_{j=1}^n (V_j^- - V_{ij})^2} \quad \text{where } i = 1, 2, 3, \dots, m, \tag{7}$$

where *i* represents criterion index and *j* represents alternative index.

Step VI—Calculate the distance between each position and the optimal solution as per Equation (8).

$$C_i = \frac{S_i^+}{s_i^+ - s_i^-}, \quad 0 \leq C_i \leq 1 \tag{8}$$

Step VII—Rank the preference order as per *C_i* values.

3. Result and Discussion

3.1. Physicomechanical Properties

The physicomechanical characteristics of the unreinforced and hybrid composites are summarized in Figure 8a–c. With the inclusion of RHA and Cu contents, the hybrid composites exhibit a slight increase in hardness and ultimate tensile strength. A significant increase in the “hardness”, “impact energy”, and “ultimate tensile strength” of hybrid composites is observed with the incorporation of RHA content, however, the effect becomes less pronounced as RHA content is increased further beyond 15 wt. %. It appears that the addition of RHA and Cu to Al-Mg-0.6Si-0.35Fe alloy with a particular weight percentage is capable of improving tensile and hardness characteristics. As the reinforcement content (RHA and Cu) increases, the elongation percentage decreases, because reinforcements are less ductile and harder than Al-Mg-0.6Si-0.35Fe alloy.

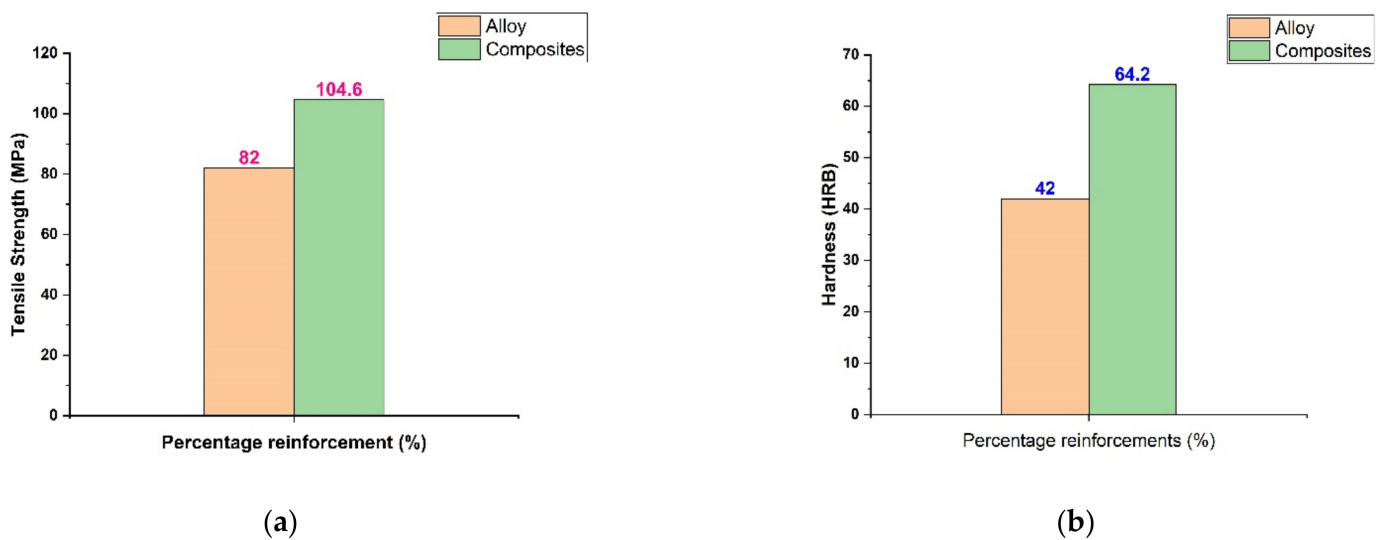
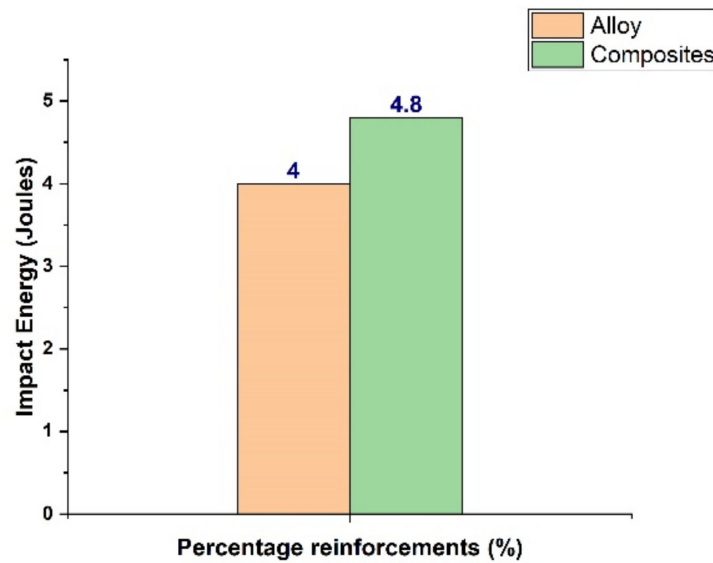


Figure 8. Cont.



(c)

Figure 8. (a) Tensile strength (MPa), (b) hardness (HRB) and (c) impact energy (joules) of the fabricated samples (Al-Mg-0.6Si-0.35Fe alloy without any reinforcing particulates, and Al-Mg-0.6Si-0.35Fe/15%RHA/5%Cu hybrid composites).

3.2. Taguchi Analysis

ANOVA for Ra reveals that interactions of pulse duration with current are the most significant factors effecting Ra, followed by peak current. However, other factors show a marginal effect on it. Table 5 shows the details.

Table 5. ANOVA table for Ra. (*significant parameters).

Source	DF	Seq SS	Adj SS	Adj MS	F	p	% Contribution
Peak current	2	28.417	15.3083	7.6542	30.6	0.032 *	23.31%
Pulse duration	2	1.988	5.3646	2.6823	10.72	0.085	1.63%
Pulse interval	2	1.182	3.2962	1.6481	6.59	0.132	0.97%
Wire feed rate	2	3.795	0.9922	0.4961	1.98	0.335	3.11%
Peak current × Pulse duration	4	36.283	35.8811	8.9703	35.86	0.027 *	29.76%
Peak current × Pulse interval	4	12.816	14.7033	3.6758	14.69	0.065	10.51%
Peak current × Wire feed rate	4	3.373	5.0738	1.2684	5.07	0.171	2.77%
Pulse duration × Pulse interval	4	33.547	33.5468	8.3867	33.52	0.029 *	27.52%
Residual error	2	0.5	0.5003	0.2502			0.41%
Total	26	121.901					

* significant parameters.

Figure 9 depicts that current of 150 A, pulse duration of 115 μs, pulse interval of 30 μs and wire feed rate of 8 mm/min are suggested as the best settings to obtain a minimum Ra value of 0.08 μm.

ANOVA for MRR (Table 6) indicates that peak current, pulse duration and pulse interval are the predominant parameters influencing MRR, which contribute 42.55%, 30.65% and 25.95%, respectively. Feed rate has a marginal effect on the MRR value.

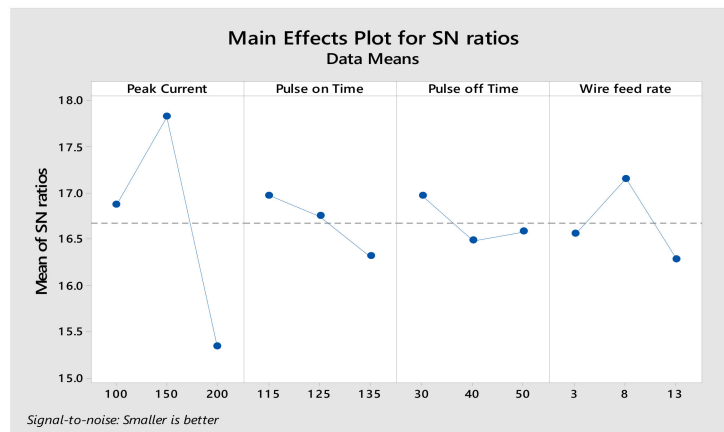


Figure 9. Main effects plot for Ra.

Table 6. ANOVA table for MRR. (*significant parameters).

Source	DF	Seq SS	Adj SS	Adj MS	F	p	% Contribution
Peak current	2	144.007	102.768	51.3841	980.51	0.001 *	25.95%
Pulse duration	2	236.167	193.986	96.9931	1850.8	0.001 *	42.55%
Pulse interval	2	170.124	146.082	73.0409	1393.8	0.001 *	30.65%
Wire feed rate	2	0.169	0.416	0.2078	3.97	0.201	0.03%
Peak current × Pulse duration	4	0.109	0.309	0.0772	1.47	0.443	0.02%
Peak current × Pulse interval	4	0.525	0.902	0.2256	4.3	0.197	0.09%
Peak current × Wire feed rate	4	2.586	0.479	0.1197	2.28	0.327	0.47%
Pulse duration × Pulse interval	4	1.235	1.235	0.3087	5.89	0.15	0.22%
Residual error	2	0.105	0.105	0.0524			
Total	26	555.027					

* significant parameters.

It is evident that at the highest levels of input parameters, a considerable amount of workpiece material is removed. This is due to the evident material removal mechanism that formed in the machining zone when a huge amount of discharge energy is supplied to the machining zone.

Figure 10 illustrates that peak current of 200 A, pulse duration of 135 μ s, pulse interval of 50 μ s and wire feed rate of 8 mm/min are suggested as the best settings to attain maximum MRR and a maximum value of 1.47 g/min is obtained.

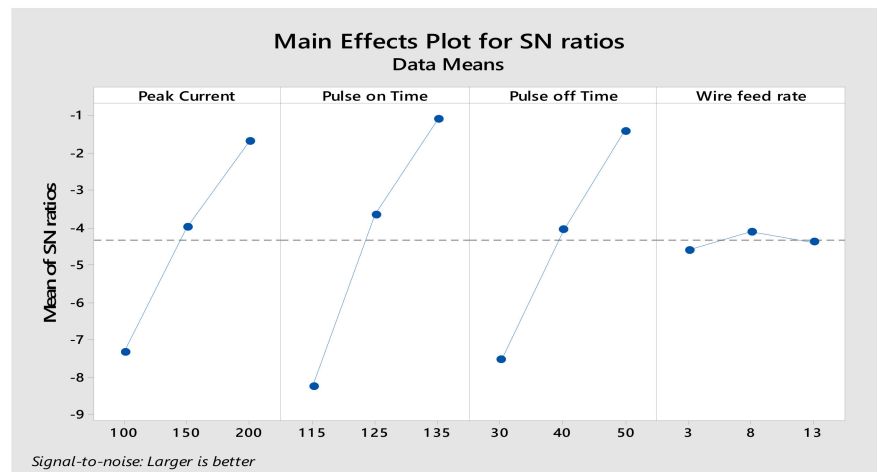


Figure 10. Main effects plot for MRR.

ANOVA for radial overcut is shown in Table 7. It indicates that current (40.10%) is the most prominent factor affecting the dimensional accuracy, followed by pulse duration (31.51%), while other factors show a marginal effect on it.

Table 7. ANOVA table for radial overcut.

Source	DF	Seq SS	Adj SS	Adj MS	F	p	% Contribution
Peak current	2	277.9	153.623	76.8116	2.83	0.261	40.16%
Pulse duration	2	218.04	151.698	75.849	2.8	0.263	31.51%
Pulse interval	2	41.086	39.185	19.5925	0.72	0.581	5.94%
Wire feed rate	2	2.375	1.793	0.8964	0.03	0.968	0.34%
Peak current × Pulse duration	4	12.122	21.517	5.3792	0.2	0.919	1.75%
Peak current × Pulse interval	4	0.987	3.739	0.9348	0.03	0.996	0.14%
Peak current × Wire feed rate	4	73.231	77.513	19.3782	0.71	0.654	10.58%
Pulse duration × Pulse interval	4	11.997	11.997	2.9994	0.11	0.967	1.73%
Residual error	2	54.225	54.225	27.1126			
Total	26	691.964					

Figure 11 illustrates that current of 100 A, pulse duration of 115 μs, pulse interval of 30 μs and wire feed rate of 3 mm/min are suggested as the best settings to attain maximum dimensional accuracy (i.e., minimum overcut) and a minimum value for radial overcut of 0.005 mm is obtained.

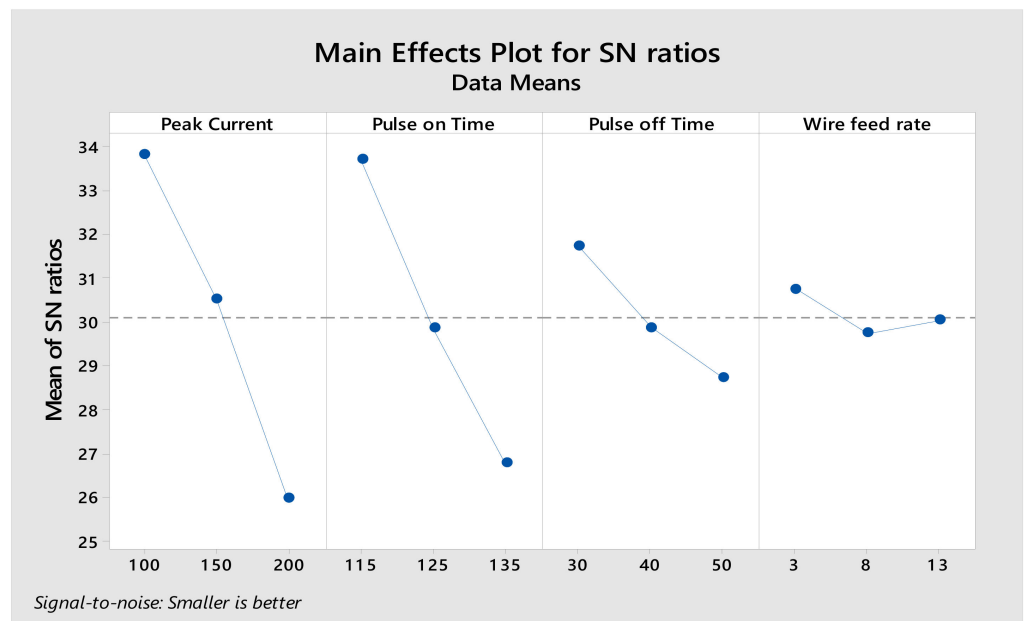


Figure 11. Main effects plot for radial overcut.

3.3. TOPSIS for Machining

In the Taguchi analysis, different sets of each response are obtained. In order to obtain optimal response characteristic parameters, TOPSIS is used, which gives one common setting to attain optimal response parameters. For this, the analysis was carried out as per the procedure mentioned in the previous section and obtained values are listed in Table 8.

Table 8. Table showing the application of TOPSIS for optimization.

Normalized Values (R_{ij})			Weighted Normalized Matrix (V_{ij})			Separation Distances		Closeness Values to the Ideal Solution	Rank
Ra	MRR	ROC	Ra	MRR	ROC	S^+	S^-	C_i	
0.136	0.047	0.032	0.045	0.015	0.011	0.133	0.148	0.527	8
0.125	0.070	0.056	0.041	0.023	0.018	0.125	0.142	0.531	5
0.137	0.090	0.102	0.045	0.030	0.034	0.121	0.127	0.511	12
0.137	0.084	0.079	0.045	0.028	0.026	0.122	0.133	0.523	9
0.187	0.118	0.134	0.062	0.039	0.044	0.117	0.112	0.488	16
0.237	0.147	0.083	0.078	0.048	0.028	0.109	0.126	0.536	4
0.225	0.104	0.167	0.074	0.034	0.055	0.128	0.098	0.433	24
0.212	0.157	0.134	0.070	0.052	0.044	0.107	0.112	0.511	13
0.237	0.225	0.171	0.078	0.074	0.057	0.096	0.108	0.528	7
0.187	0.068	0.097	0.062	0.022	0.032	0.130	0.122	0.485	18
0.162	0.107	0.060	0.054	0.035	0.020	0.115	0.137	0.544	2
0.137	0.136	0.125	0.045	0.045	0.041	0.108	0.121	0.529	6
0.162	0.121	0.083	0.054	0.040	0.028	0.111	0.130	0.540	3
0.162	0.166	0.158	0.054	0.055	0.052	0.103	0.111	0.518	10
0.175	0.235	0.232	0.058	0.078	0.076	0.099	0.099	0.501	14
0.187	0.152	0.190	0.062	0.050	0.063	0.114	0.097	0.460	21
0.200	0.217	0.269	0.066	0.072	0.089	0.113	0.084	0.425	25
0.112	0.327	0.158	0.037	0.108	0.052	0.058	0.142	0.711	1
0.275	0.086	0.130	0.091	0.028	0.043	0.135	0.107	0.442	23
0.212	0.137	0.260	0.070	0.045	0.086	0.132	0.073	0.355	27
0.287	0.176	0.153	0.095	0.058	0.050	0.114	0.106	0.481	19
0.137	0.161	0.283	0.045	0.053	0.093	0.126	0.081	0.392	26
0.225	0.217	0.181	0.074	0.072	0.060	0.098	0.105	0.517	11
0.250	0.294	0.264	0.082	0.097	0.087	0.103	0.098	0.489	15
0.187	0.179	0.213	0.062	0.059	0.070	0.110	0.094	0.459	22
0.237	0.314	0.301	0.078	0.104	0.099	0.108	0.097	0.474	20
0.162	0.449	0.454	0.054	0.148	0.150	0.140	0.132	0.486	17

ANOVA for C_i reveals that current is the most predominant parameter influencing response characteristic parameters and contributes 24.09% to attaining optimal machining characteristics, followed by pulse duration (16.78%) and pulse interval (15.18%), as shown in Table 9. Feed rate shows a marginal effect on the response characteristic parameters.

Table 9. ANOVA for C_i .

Source	DF	Seq SS	Adj SS	Adj MS	F	p	% Contribution
Peak current	2	7.4998	3.6819	1.841	0.44	0.695	24.09%
Pulse duration	2	5.2247	0.6098	0.3049	0.07	0.932	16.78%
Pulse interval	2	4.7243	3.3891	1.6946	0.4	0.712	15.18%
Wire feed rate	2	1.403	0.4998	0.2499	0.06	0.944	4.51%
Peak current × Pulse duration	4	2.0193	2.9795	0.7449	0.18	0.931	6.49%
Peak current × Pulse interval	4	0.8156	1.1666	0.2917	0.07	0.985	2.62%
Peak current × Wire feed rate	4	4.4209	4.0696	1.0174	0.24	0.893	14.20%
Pulse duration × Pulse interval	4	2.8961	2.8961	0.724	0.17	0.934	9.30%
Residual error	2	2.3908	8.3908	4.1954			7.68%
Total	26	31.1318					

Figure 12 illustrates that peak current of 150 A, pulse duration of 125 μ s, pulse interval of 50 μ s and wire feed rate of 8 mm/min are suggested as the optimum set of input conditions to attain optimal dimensional accuracy, surface roughness and material removal rate.

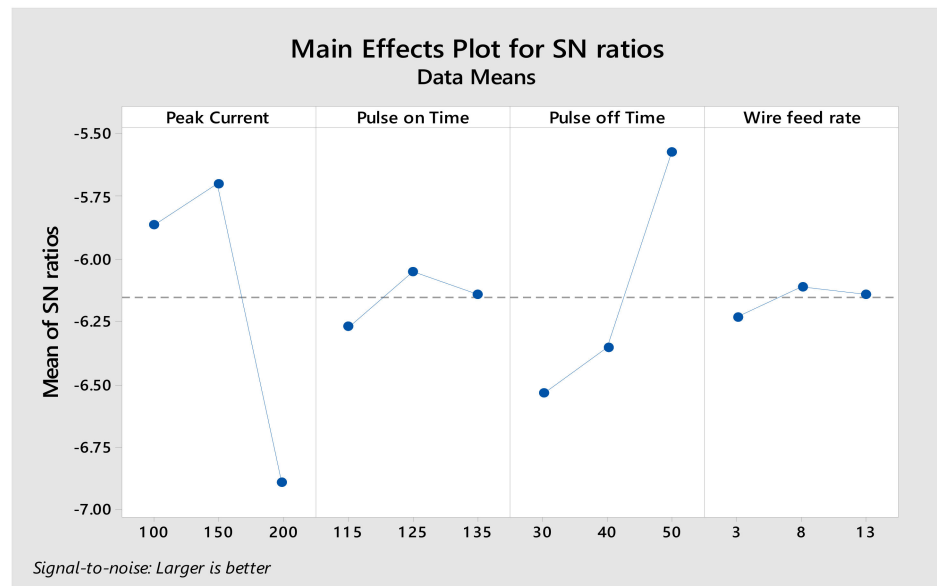


Figure 12. Main effects plot for C_i .

3.4. Confirmatory Experimentation

After the application of TOPSIS, the optimum setting for response parameters was suggested and the confirmation experiment was performed accordingly. Predicted performance index was evaluated according to Equation (9) [35].

$$C_i \text{ (predicted)} = \text{mean of } A_2 + \text{mean of } B_2 + \text{mean of } C_3 + \text{mean of } D_2 - 4 \text{ mean of } C_i \text{ (9)}$$

Table 10 shows the initial process parameter ($A_2B_3C_3D_2$) set of “material removal rate, surface roughness and radial overcut” and corresponding C_i value. This table also indicates the comparison of the predicted performance index with its experimental value.

Table 10. Results of machining responses as per initial and optimal machining parameters.

Responses	Initial Parameter $A_2B_3C_3D_2$	Optimum Parameters	
		Predicted $A_2B_2C_3D_2$	Experimental $A_2B_2C_3D_2$
Material removal rate (g/min)	0.09		0.08
Surface roughness (μm)	1.336		1.429
Radial overcut (mm)	0.034		0.030
Performance index (C_i)	0.7109	0.7501	0.7601

Furthermore, the projected performance index was compared to the experimental performance index to determine the percentage error as per Equation (10).

$$\% \text{ Error} = \frac{C_{i(\text{Experimental})} - C_{i(\text{Predicted})}}{C_{i(\text{Predicted})}} \times 100 \tag{10}$$

It has been observed that % error obtained from the above equation is equal to 1.33%, which indicates the results are validated and means the values obtained after confirmatory experiments are optimal values. Furthermore, a significant improvement in the performance index (around 0.0492) is also obtained compared to the initial parameter setting ($A_2B_3C_3D_2$), when the experiments were conducted according to suggested optimal parameter settings by employing TOPSIS. Therefore, the result of confirmation experiments shows significant improvements in the surface finishing, material removal rate and dimensional inaccuracy. The optimal balanced values are MRR = 1.35 g/min, Ra = 0.08 μm and

ROC = 0.032 mm. A similar result was revealed by Chinmayee et al. [31], who conducted a study to investigate the machining parameters of Al7075 6% red mud MMC in the electric discharge machine (EDM) process after experiments were conducted using the central composite design of the experimentation. It has been found that in comparison with the other inputs, i.e., Pon-time and gap voltage, the peak current exerts a major impact on the responses. ANOVA findings and values of correlation coefficients indicated a strong predictive power for the response models of the non-linear regression. In addition, the confirmation test for the regression models was also conducted with the help of 10 observational test cases, which were separate from the data, used to fit the regression model. Satpathy et al. [32] focused on multiple objective optimizations of EDM for Al-20%SiC composite using TOPSIS. It was found that SR increases with an increase in peak current, and it decreases with an increase in Pon-time. The surface roughness remains constant up to a certain limit of gap voltage and then increases suddenly when gap voltage further increases beyond this limit. Dharmalingam et al. [33] also explored the effect of input controllable factors during electrochemical machining of Al-SiC-B₄C hybrid composite and concluded that electrolytic concentration and voltage are the most substantial variables for MRR, whereas electrolytic concentration is a significant factor for overcut. Manish et al. [34] explored the effect of reinforcement contents and machining parameters during EDM of Al (LM6)-SiC-B₄C hybrid MMCs. The authors observed that current is the most influential factor for MRR, and for TWR and ROC, peak current is the main affecting variable, followed by Pon-time, and the other parameters are insignificant.

The SEM images of hybrid AMC, taken prior to and after machining (as per the best set of input conditions obtained from TOPSIS), are shown in Figure 13a–c. Images depict significant improvements in surface quality, when machined using optimized input conditions suggested by TOPSIS.

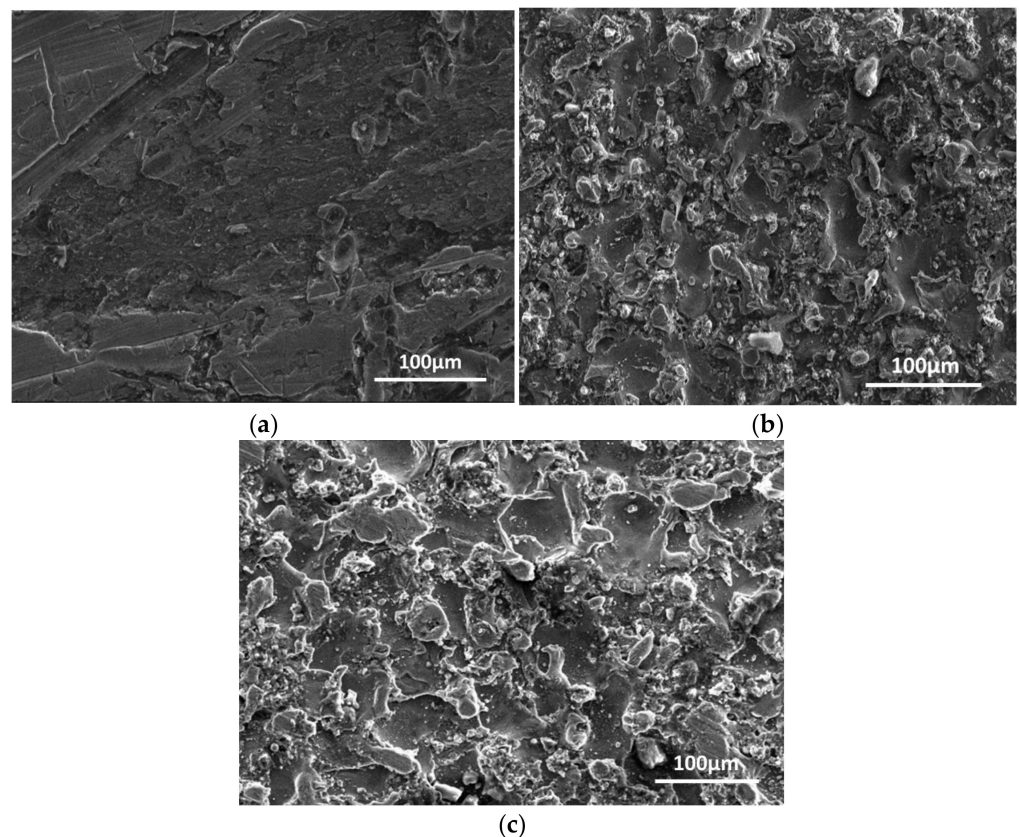


Figure 13. SEM images of AMC, (a) before machining at 250×; (b) machined surface as per best setting for maximum MRR at 250×; and (c) machined surface as per best setting for minimum overcut at 250×.

Thus, the microstructure of MMCs is an essential property, which describes the quality of the composite materials. It also illustrates the effectiveness of the fabrication method used for the production. Generally, for homogeneity, the reinforcement's particles should be distributed uniformly within the matrix material, and should not be agglomerated/seggregated during solidification. The overall characteristic profile of the composites depends upon the type of reinforcement particles, their morphology and dispersion of reinforcements in the matrix metal/alloy. Furthermore, the dispersion of reinforcement particles generally depends on the type of reinforcement used, the fluidity of the melt while pouring, the method of incorporating reinforcements in the matrix, solidification rate and wettability property of the constituents. The addition of Mg has an important effect on the wettability of the particles in molten states. Onoro [26] conducted a study of the tensile properties and fracture properties of composites strengthened by TiB₂. These materials were investigated at room temperature and at high temperatures for the identification of ultimate strength and strain to failure. An improvement in the mechanical behavior was achieved by adding TiB₂ particles in both the Al alloys as reinforcement. The research concluded that adding TiB₂ particles decreases the ductility of the Al alloys but does not change the microscopic failure mechanism, and the surface of the fracture exhibits a ductile impression with coalescence-formed dimples. Dursun et al. [36] analyzed the microstructure of newly developed Al-15%SiC composite, which was fabricated by the thixo molding process at a processing temperature of 590 °C, and observed a spherical grain structure formed in the composite. Walczak et al. [37] analyzed the influence of T6 heat treatment and the addition of SiC in the microstructure of AlSi9Mg alloy matrix and found that T6 heat treatment does not cause any significant changes in base matrices and their composites. In addition, the SiC was distributed uniformly throughout the matrix material. Elango and Raghunath [38] studied the effect of the addition of reinforcements (SiC and TiO₂) on the microstructure of aluminum (LM25) alloy matrix material fabricated by the stir casting route. The authors observed a uniform dispersion of reinforcing phase in the base metal/alloy together with refining of grain size and rising porosity with respect to TiO₂ contents.

4. Conclusions

On the basis of experimental observations made on the fabrication and evaluation of machining behavior of novel Al-Mg-0.6Si-0.35Fe/15%RHA/5%Cu hybrid composite, the following conclusions can be drawn:

- i. The stir casting method can be successfully adopted for the fabrication of Al-Mg-0.6Si-0.35Fe/15%RHA/5%Cu hybrid composites. The composite exhibits hardness of 64.2 HRB, tensile strength 104.6 MPa, impact energy 4.8 joules, when tested using standard testing techniques.
- ii. The SEM and EDS results confirm aluminum as a main constituent, and Si as a major alloying element, and the other alloying elements are also present accordingly. The existence of alloying elements in aluminum alloy is validated using spark electromagnetic analysis. X-ray diffraction analysis has been performed to recognize secondary compound formation resulting from internal reactions. An optical microscope with an image analyzer was also utilized to evaluate microstructural behavior.
- iii. Results of Taguchi analysis reveal that interactions between pulse duration and peak current, as well as pulse interval, are the most relevant factors affecting surface roughness, followed by peak current. Other variables, on the other hand, have a small influence on it. The peak current, pulse duration and pulse interval are the most prominent factors for MRR that contribute 42.55%, 30.65% and 25.95%, respectively, while feed rate has a small impact on it. The results for radial overcut reveal that current (40.10%) has the largest impact on dimensional accuracy, followed by pulse duration (31.51%), with other variables having only a slight impact.
- iv. The consequences of TOPSIS analysis reveal that current is the most predominant parameter influencing response characteristic parameters and contributes 24.09% to attaining optimal machining characteristics, followed by pulse duration (16.78%) and

pulse interval (15.18%). Radial overcut indicates that current (40.10%) is the most prominent factor effecting the dimensional accuracy, followed by pulse duration (31.51%), while other factors show a marginal effect on it. Additionally, current of 150 A, pulse duration of 125 μ s, pulse interval of 50 μ s and wire feed rate of 8 mm/min are suggested as the optimum set of input conditions to attain optimal dimensional accuracy, surface roughness and material removal rate. A confirmatory test reveals that predicted performance index is very close to the experimental performance index value (%error = 1.33% only) which validates the obtained results. In addition, a significant improvement in the performance index was also obtained (around 0.0492) over initial input parameters settings when compared to the optimal parameter setting. Therefore, optimal values of response characteristics are MRR = 1.35 g/min, Ra = 0.08 μ m and ROC = 0.032 mm. The SEM images of hybrid AMC depict significant improvements in surface quality, when machined using optimized input conditions.

Author Contributions: Conceptualization, J.K., S.S. (Shubham Sharma) and J.S.; methodology, J.K., S.S. (Shubham Sharma) and J.S.; formal analysis, J.K., S.S. (Shubham Sharma) and J.S.; investigation, J.K., S.S. (Shubham Sharma) and J.S.; writing—original draft preparation, J.K., S.S. (Shubham Sharma) and J.S.; writing—review and editing, S.S. (Shubham Sharma), S.S. (Sunpreet Singh) and G.S.; supervision, S.S. (Shubham Sharma), S.S. (Sunpreet Singh) and G.S.; project administration, S.S. (Shubham Sharma) and G.S.; funding acquisition, S.S. (Shubham Sharma) and G.S. All authors have read and agreed to the published version of the manuscript.

Funding: This research received no external funding.

Institutional Review Board Statement: Not applicable.

Informed Consent Statement: Not applicable.

Data Availability Statement: No data were used to support this study.

Conflicts of Interest: The authors declare no conflict of interest.

References

1. Koshy, P.; Jain, V.K.; Lal, G.K. Experimental investigations into electrical discharge machining with a rotating disk electrode. *J. Precis. Eng.* **1993**, *15*, 6–15. [[CrossRef](#)]
2. Hung, N.P.; Yang, L.J.; Leong, K.W. Electrical Discharge Machining of Cast Metal Matrix Composites. *J. Mater. Process. Technol.* **1994**, *44*, 229–236. [[CrossRef](#)]
3. Tarnag, Y.S.; Ma, S.C.; Chung, L.K. Determination of optimal cutting parameters in wire electrical discharge machining. *Int. J. Mach. Tools Manuf.* **1995**, *35*, 1693–1700. [[CrossRef](#)]
4. Wang, C.C.; Yan, B.H. Blind-hole drilling of Al₂O₃/6061 Al composite using rotary electro discharge machining. *J. Mater. Process. Technol.* **2000**, *102*, 90–102. [[CrossRef](#)]
5. Rozenek, M.; Kozak, J.; Dabrowski, L.; Lubkowski, K. Electrical Discharge Machining Characteristics of Metal Matrix Composites. *J. Mater. Process. Technol.* **2001**, *109*, 367–370. [[CrossRef](#)]
6. Mahapatra, S.S.; Patnaik, A. Parametric Optimization of WEDM Process Using Taguchi Method. *J. Braz. Soc. Mech. Sci. Eng.* **2006**, *28*, 422–429. [[CrossRef](#)]
7. Han, F.; Jiang, J.; Yu, D. Influence of machining parameters on surface roughness in finish cut of WEDM. *Int. J. Adv. Manuf. Technol.* **2007**, *34*, 538–546. [[CrossRef](#)]
8. Lin, Y.C.; Chena, Y.F.; Wang, D.A.; Lee, H.-S. Optimization of machining parameters in magnetic force assisted EDM based on Taguchi method. *J. Mater. Process. Technol.* **2009**, *209*, 3374–3383. [[CrossRef](#)]
9. Sari, M.M.; Noordin, M.Y.; Brusa, E. Role of multi-wall carbon nanotubes on the main parameters of the electrical discharge machining (EDM) process. *Int. J. Adv. Manuf. Technol.* **2013**, *68*, 1095–1102. [[CrossRef](#)]
10. Syed, K.H.; Kuppan, P. Studies on Recast-layer in EDM using Aluminium Powder Mixed Distilled Water Dielectric Fluid. *Int. J. Eng. Technol.* **2013**, *5*, 1775–1780.
11. Kanlayasiri, K.; Jattakul, P. Simultaneous optimization of dimensional accuracy and surface roughness for finishing cut of wire EDMed K460 tool steel. *Precis. Eng.* **2013**, *37*, 556–561. [[CrossRef](#)]
12. Yeh, C.-C.; Wu, K.-L.; Lee, J.-W.; Yan, B.-H. Study on surface characteristics using phosphorous dielectric on wire electrical discharge machining of polycrystalline silicon. *Int. J. Adv. Manuf. Technol.* **2013**, *69*, 71–80. [[CrossRef](#)]
13. Rajesha, S.; Jawalkar, C.S.; Mishra, R.R.; Sharma, A.K.; Kumar, P. Study of recast layers and surface roughness on Al-7075 metal matrix composite during EDM machining. *Int. J. Recent Adv. Mech. Eng.* **2014**, *3*, 53–62.

14. Jangra, K.; Grover, S.; Aggarwal, A. Optimization of multi machining characteristics in WEDM of WC-5.3% Co composite using integrated approach of Taguchi, GRA and entropy method. *Front. Mech. Eng.* **2012**, *7*, 288–299. [[CrossRef](#)]
15. Akash, R.; Muraliraja, R.; Suthan, R.; Shaisundaram, V.S. Synthesis and testing of aluminium composite using industrial waste as reinforcement. *Mater. Today Proc.* **2021**, *37*, 634–637. [[CrossRef](#)]
16. Joseph, J.D.; Kumaragurubaran, B.; Sathish, S. Effect of MoS₂ on the Wear Behavior of Aluminium (AlMg0.5Si) Composite. *Silicon* **2019**, *12*, 1–9. [[CrossRef](#)]
17. Ho, K.H.; Newman, S.T. State of the art electrical discharge machining (EDM). *Int. J. Mach. Tools Manuf.* **2003**, *43*, 1287–1300. [[CrossRef](#)]
18. Shu, K.M.; Tu, G.C. Study of electrical discharge grinding using metal matrix composite electrodes. *Int. J. Mach. Tools Manuf.* **2003**, *43*, 845–854. [[CrossRef](#)]
19. Simao, J.; Lee, H.G.; Aspinwall, D.K.; Dewes, R.C.; Aspinwall, E.M. Workpiece surface modification using electrical discharge machining. *J. Mater. Process. Technol.* **2003**, *43*, 121–128. [[CrossRef](#)]
20. Aharwal, K.R.; Krishna, C.M. Optimization of material removal rate and surface roughness in EDM machining of metal matrix composite using genetic algorithm. *Mater. Today* **2018**, *5*, 5391–5397. [[CrossRef](#)]
21. Onoro, J. High temperature mechanical properties of aluminum alloys reinforced with titanium diboride (TiB₂) particles. *Rare Met.* **2011**, *30*, 200–205. [[CrossRef](#)]
22. Parashar, V.; Rehman, A.; Bhagoria, J.L.; Puri, Y.M. Investigation and Optimization of Surface Roughness for Wire Cut Electro Discharge Machining of SS 304L using Taguchi Dynamic Experiments. *Int. J. Eng. Stud.* **2009**, *1*, 257–267.
23. Saha, S.K.; Choudhury, S.K. Experimental investigation and empirical modeling of the dry electric discharge machining process. *Int. J. Mach. Tools Manuf.* **2009**, *49*, 297–308. [[CrossRef](#)]
24. Mahdavejad, R.A. Optimization of electro discharge machining parameters. *J. Achiev. Mater. Manuf. Eng.* **2008**, *27*, 163–166.
25. Patel Gowdru Chandrashekarappa, M.; Kumar, S.; Pimenov, D.Y.; Giasin, K. Experimental Analysis and Optimization of EDM Parameters on HcHcr Steel in Context with Different Electrodes and Dielectric Fluids Using Hybrid Taguchi-Based PCA-Utility and CRITIC-Utility Approaches. *Metals* **2021**, *11*, 419. [[CrossRef](#)]
26. Sen, B.; Hussain, S.A.I.; Gupta, A.D.; Gupta, M.K.; Pimenov, D.Y.; Mikołajczyk, T. Application of Type-2 Fuzzy AHP-ARAS for Selecting Optimal WEDM Parameters. *Metals* **2021**, *11*, 42. [[CrossRef](#)]
27. Aggarwal, V.; Pruncu, C.I.; Singh, J.; Sharma, S.; Pimenov, D.Y. Empirical Investigations during WEDM of Ni-27Cu-3.15 Al-2Fe-1.5 Mn Based Superalloy for High Temperature Corrosion Resistance Applications. *Materials* **2020**, *13*, 3470. [[CrossRef](#)] [[PubMed](#)]
28. Kumar, J.; Singh, D.; Kalsi, N.S.; Sharma, S.; Mia, M.; Singh, J.; Rahman, M.A.; Khan, A.M.; Rao, K.V. Investigation on the Mechanical, Tribological, Morphological and Machinability behavior of stir-casted Al/SiC/Mo reinforced MMCs. *J. Mater. Res. Technol.* **2021**, *12*, 930–946. [[CrossRef](#)]
29. Kumar, J.; Singh, D.; Kalsi, N.S.; Sharma, S.; Pruncu, C.I.; Pimenov, D.Y.; Rao, K.V.; Kapłonek, W. Comparative study on the mechanical, tribological, morphological and structural properties of vortex casting processed, Al-SiC-Cr hybrid metal matrix composites for high strength wear-resistant applications: Fabrication and characterizations. *J. Mater. Res. Technol.* **2020**, *9*, 13607–13615. [[CrossRef](#)]
30. Shaikh, N.; Bilal, M.; Sajjad, A.; Tariq, A.; Adnan, W.; Mohd, S.; Mohammed, A. Microstructural, mechanical and tribological behaviour of powder metallurgy processed SiC and RHA reinforced Al-based composites. *Surf. Interfaces* **2019**, *15*, 166–179. [[CrossRef](#)]
31. Chinmayee, K.; Surekha, B.; Hemalatha, J.; Suvan, D.C. Study of Influence of Process Parameters in Electric Discharge Machining of Aluminum—Red Mud Metal Matrix Composite. *Procedia Manuf.* **2018**, *20*, 392–399. [[CrossRef](#)]
32. Avijeet, S.; Tripathy, S.; Pallavi, S.N.; Mihir, B. Optimization of EDM process parameters for AlSiC-20% SiC reinforced metal matrix composite with multi response using TOPSIS. *Mater. Today: Proc.* **2017**, *4*, 3043–3052. [[CrossRef](#)]
33. Dharmalingam, S.; Babu, B.; Raja, R.K.; Udhataraj, S.; Vairamani, V. Electrochemical Micro Machining on Hybrid Metal Matrix Composites. *Int. J. Chem. Tech. Res.* **2015**, *8*, 508–518.
34. Manish, S.; Pankaj, A.; Mohan, P.; Dhakad, S. Experimental Investigation of EDM Parameters on Al-LM6/SiC/B4C Hybrid Composites. *Appl. Mech. Mater.* **2018**, *877*, 2017–2022. [[CrossRef](#)]
35. Zeng, Y.P.; Lin, C.L.; Dai, H.M.; Lin, Y.C.; Hung, J.C. Multi-performance optimization in electrical discharge machining of Al₂O₃ ceramics using Taguchi base AHP weighted TOPSIS method. *Processes* **2021**, *9*, 1647. [[CrossRef](#)]
36. Dursun, Ö.; Ali, K.; Musa, Y.; Tansel, T.; İbrahim, Ç. Experimental investigation and prediction of wear properties of Al/SiC metal matrix composites produced by thixomoulding method using Artificial Neural Networks. *Mater. Des.* **2014**, *63*, 270–277. [[CrossRef](#)]
37. Walczak, M.; Daniel, P.; Zwierzchowski, M. The tribological characteristics of SiC particle reinforced aluminium composites. *Arch. Civ. Mech. Eng.* **2014**, *15*, 116–123. [[CrossRef](#)]
38. Elango, G.; Raghunath, B.K. Tribological behavior of hybrid (LM25Al + SiC + TiO₂) metal matrix composites. *Procedia Eng.* **2013**, *64*, 671–680. [[CrossRef](#)]